

# Low Power RF Interface of the Near-field Communications Tag IC for Sensors

In-Young Lee<sup>1</sup> and Donggu Im<sup>2</sup>

**Abstract**—In this paper, we propose the RF interface of NFC tag IC which is necessary for transmitting the results obtained using blood glucose sensor, water quality sensor, gas sensor and radioactive sensor to portable devices such as mobile phones. The proposed RF interface complies with the ISO14443 type-A standard using 100% ASK and solves the power and clock generation difficulties by using the internal  $V_{TH}$  canceling rectifier that is based on the high efficiency voltage doubler and the switching phase locked loop. In the measurement results, the internal  $V_{TH}$  canceling rectifier in the RF interface shows more than 80% power efficiency from 100% ASK signal, and successfully generates 1.8 V / 2.5 V supply from the input signal power higher than 6 dBm through low loss voltage regulator. Additionally, we can verify that the proposed switching phase locked loop is locked at 8 dBm or higher input signal power and successfully demodulates ASK input signal.

**Index Terms**—Near-field communication, RFID, tag IC, voltage doubler, phase-locked loop, passive transponder

## I. INTRODUCTION

While RFID technology is widely distributed recently, it has been utilized in a wide range of area such as management of logistics and supply chain, portable health care unit, contactless payment system, on-board biomedical system in the human body, and architecture access control system etc. The design of low-cost transponder is required for the management of logistics and supply chain while miniaturization is essential for insertion into the human body in the case of biomedical system. For a passive transponder, there are difficulties that not only working area is limited but also it has to be satisfied with both low power consumption and secure of operating area at once since it operates without battery [6]. Passive transponders can operate at LF band (135 kHz), HF band (13.56 MHz), UHF band (860~960 MHz) and microwave band (~2.45 GHz). For LF and HF band of them, it can work through inductive coupling in the near magnetic field while it work based on a long distance electromagnetic wave for UHF and microwave band. Communications between readers and transponders are divided into uplink and downlink. Transponders generate and transmit the modulated signal in the downlink while it executes load modulation (LF, HF) or backscatter modulation (UHF) in the uplink. Since the power generation is not easy in downlink and thus the transmission distance is limited, the rectifiers based on voltage doubler are generally used to overcome this. Also, it's desirable to use RF clamps (RF limiter) to protect the transponder from overvoltage situation in the strong field. According to ISO14443 standard, for type-A, readers use 100% ASK modulation system to commute with transponders [1-3] while 10% ASK modulation is used

---

Manuscript received Nov. 16, 2022; reviewed Jan. 22, 2023; accepted Feb. 10, 2023

<sup>1</sup>Department of Electronic Engineering, Chosun University, Gwangju 61452, Korea.

<sup>2</sup>Division of Electronics Engineering, Jeonbuk National University, Jollabuk-do 561-756, Korea  
E-mail : dgim@jbnu.ac.kr

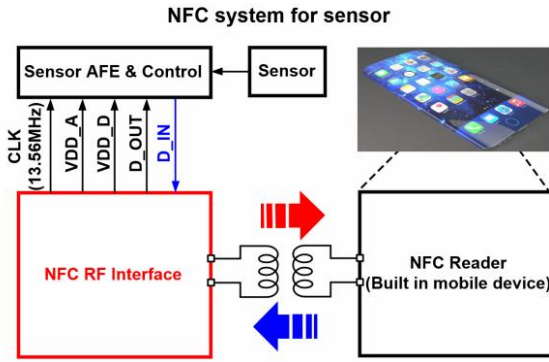


Fig. 1. The block diagram of the near field communication system for sensors.

for type-B [4, 5]. In case of type-A, it is relatively easy to sense signals while the efficiency of supply power generation is low and it is difficult to generate clock to operate digital block [7]. On the other hand, for type-B, it is easy to generate supply power and clock while signal sensing becomes difficult, especially under PVT variation condition [6, 8]. In this paper, we adopts the internal  $V_{TH}$  canceling rectifier [9] based on voltage doubler whose power conversion efficiency is high enough to overcome the difficulty of supply generation in ISO 14443 type-A. Additionally, we propose a RF interface structure complementing all drawbacks by proposing the loop-adjustable PLL which allows to generate a stable clock despite 100% ASK signal.

The remainder of this paper is organized as follows. Section II describes the proposed RF interface based on the high efficiency rectifier, the loop-adjustable PLL and their operational principles. Section III shows the experimental results for the implemented RF interface and section IV concludes the paper.

## II. PROPOSED RF INTERFACE BASED ON HIGH EFFICIENCY RECTIFIER AND LOOP-ADJUSTABLE PLL

Fig. 1 depicts the block diagram of the near field communication (NFC) system for sensors. As shown in the Fig. 1, NFC reader generates an induced current to the RF interface as the way generating the magnetic field from the initial inner coil (LF, HF) or radiating the magnetic field through backscatter (UHF). By rectifying this current the RF interface generates the supply voltages (VDD\_A and VDD\_D) that are required to

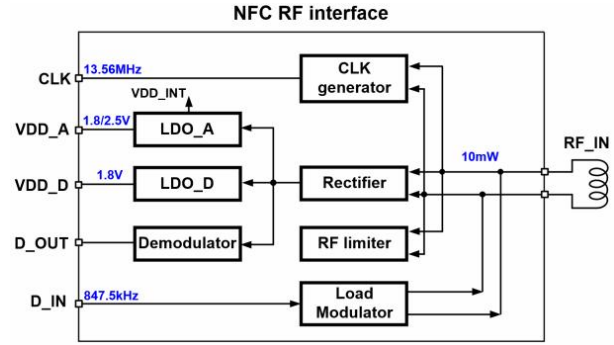


Fig. 2. The block diagram of the proposed RF interface.

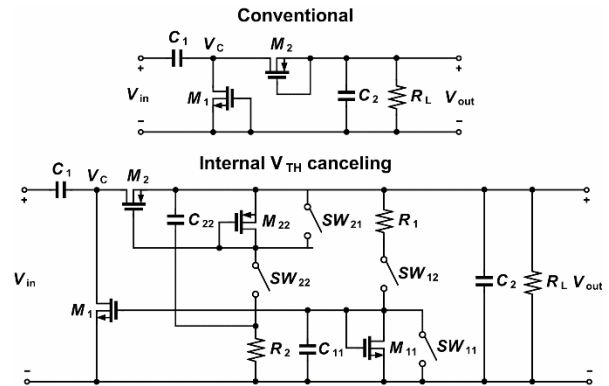


Fig. 3. The schematics of the rectifiers that adopts the conventional and the internal  $V_{TH}$  canceling structures.

operate the circuits in the RF interface, sensor analog front-end (AFE) and the control unit. At this time, the data recognized by the sensor is transformed into the electrical signal (D\_IN) through the sensor AFE and then it is transmitted to the RF interface. Fig. 2 depicts the block diagram of the proposed RF interface. As shown in the Fig. 2, the RF interface consists of a clock generator, a rectifier, a RF limiter, a load modulator, low-dropout regulators (LDO), and a demodulator. From RF\_IN, the rectifier generates supply voltages for LDO, demodulator, and CLK generator. LDO generates 1.8 V and 2.5 V for the analog and digital supplies of the sensor AFE and the control unit respectively. The demodulator demodulates and transmits the received data to the sensor AFE. The proposed NFC RF interface adopts a high efficiency rectifier based on the voltage doubler to generate the stable supply in a weak field. Besides, for the stable clock generation against inconsistent input data (D\_IN) and thus to satisfy ISO14443 type-A, the phase locked loop (PLL) is designed to be loop-adjustable, which allows the PLL loop only turns on when the input data is

'1'. Fig. 3 depicts the schematics of the rectifiers that adopt the conventional and the internal  $V_{TH}$  canceling structures respectively. For the rectifier that adopts the conventional voltage doubler, the magnitude of output voltage is limited by  $2V_{in} - (V_{TH,N} - V_{TH,P})$  because it uses two diode-connected transistors where  $V_{TH,N}$  and  $V_{TH,P}$  are the threshold voltages of n- and p-MOSFET, respectively. Therefore, the conventional structure makes it difficult to generate the required supply in a weak field. On the other hand, for the internal  $V_{TH}$  canceling (IVC) structure, it minimizes the the output voltage loss caused by the threshold voltage and furthermore lowers the effective threshold voltage of transistors by using four switches ( $SW_{11}$ ,  $SW_{12}$ ,  $SW_{21}$  and  $SW_{22}$ ) based on IVC system [9, 10]. This enhances the power conversion efficiency by minimizing reverse leakage current with applying a voltage pulse instead of constant voltage to the transistor gate unlike the previous IVC technique [10]. As shown in the Fig. 3, there are two IVC cells and hence a total of four switches ( $SW_{11}$ ,  $SW_{12}$ ,  $SW_{21}$  and  $SW_{22}$ ) are needed. In the first cell, since  $SW_{11}$  is 'off' and  $SW_{12}$  is 'on' while  $M_1$  is 'on', it shows general IVC operation as the constant voltage is applied to the  $M_1$  gate. Meanwhile, when  $SW_{11}$  turns 'on' and  $SW_{12}$  turns 'off' while  $M_1$  is 'off', the IVC cell is disconnected with  $M_1$  gate and  $M_1$  gate is grounded through  $SW_{11}$ . In this process, the gate voltage of  $M_1$  is applied as the form of pulse,  $V_{G1}$ , where its amplitude is  $0 \sim V_{TH,N}$ . For  $M_2$ , the pulse form of  $V_{G2}$  is applied in the same way.

Fig. 4 depicts the simulated output voltage waveforms of the conventional and the internal  $V_{TH}$  canceling structures. As shown in the Fig. 4, in the conventional structure, the constant voltage is applied to the transistor gate and it generates 0.55 V output voltage based on 1 V peak-to-peak sine wave input. Meanwhile, for the proposed IVC structure, the pulse form of voltage is applied to the transistor gate and hence it generates 0.9 V output voltage under the same conditions, which means the power conversion efficiency (PCE) is improved from 49% to 80%.

Fig. 5 is the block diagram of the proposed low power PLL to generate a stable clock from the 100% ASK input signal as a reference clock. Since the reference frequency ( $f_{REF}$ ) and VCO frequency ( $f_{VCO}$ ) are same, the PLL is designed in a integer type. Basically, since 100% ASK signal shows no signal when the data is '0', it is obvious

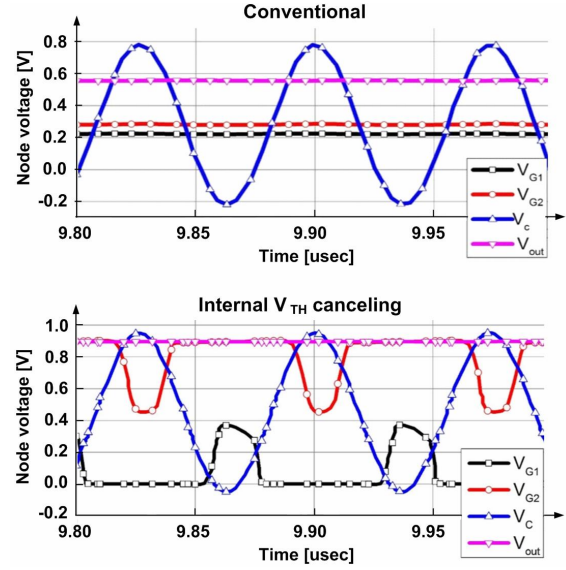


Fig. 4. The simulated output voltage waveforms of the conventional and the internal  $V_{TH}$  canceling structures.

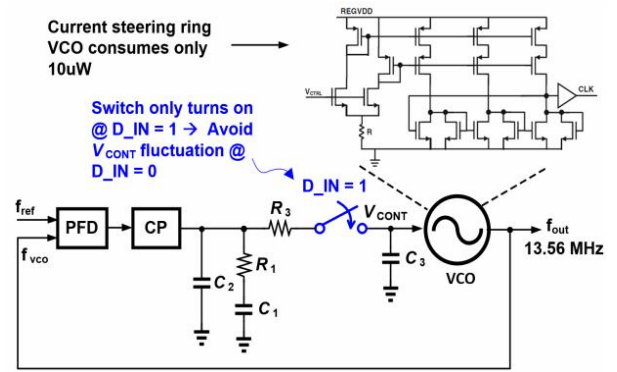


Fig. 5. The block diagram of the proposed low power PLL.

that PLL can not be locked steadily. In order to solve this issue, we propose the switched loop PLL. The PLL loop is only closed when the received ASK signal is '1'. Otherwise, the loop is switched off and keeps the electric charge that has already been charged on the capacitor ( $C_3$ ) at the edge of the loop filter, thus allowing the VCO to generate the locked frequency. Additionally, the proposed PLL employs a current steering type of ring VCO [11] for a low power implementation as seen in Fig. 5 and it only consumes less than 10  $\mu$ W.

Fig. 6 depicts the block diagram of the demodulator and the schematic of the envelope detector. The envelope detector is simply designed with a total of four transistors where  $M_1$  plays the role of a rectifier using diode-connection, and  $M_2$  acts as a capacitor.  $M_3$  and  $M_4$  minimize the leakage current by using diode-connected

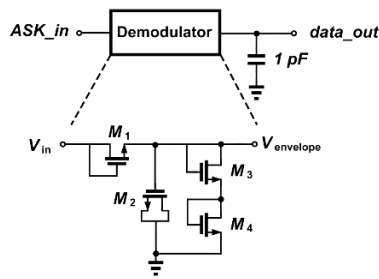


Fig. 6. The block diagram of the demodulator and the schematic of the envelope detector.

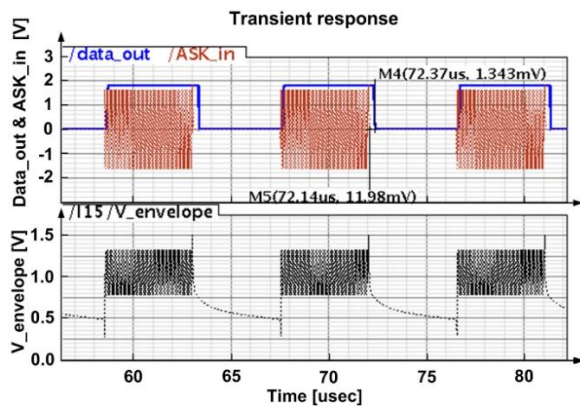


Fig. 7. The simulated output waveform of the demodulator.

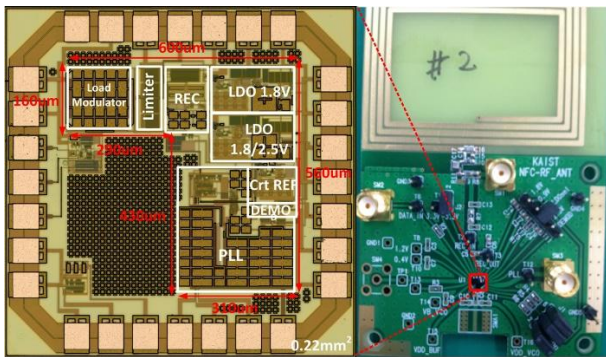


Fig. 8. The micrograph of the proposed RF interface chip and the photo of the implemented NFC tag with an external coil.

transistors instead of resistors. The simulation results with 1 pF capacitor in the load are shown in Fig. 7, which verify that the output of envelope detector ( $V_{envelope}$ ) and demodulated output ( $data\_out$ ) come out properly on the 100% ASK input signal ( $ASK\_in$ ).

### III. EXPERIMENTAL RESULTS

Fig. 8 shows the micrograph of the proposed RF interface chip and the photo of the implemented NFC tag

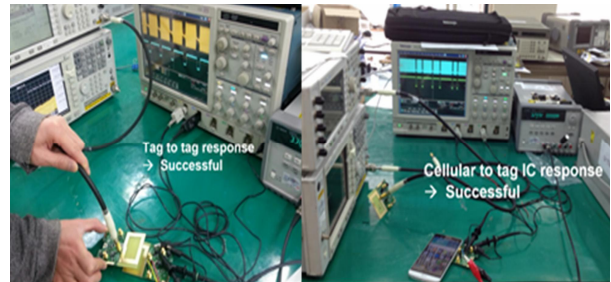


Fig. 9. The demonstration of tag-to-tag and cellular phone-to-tag responses.

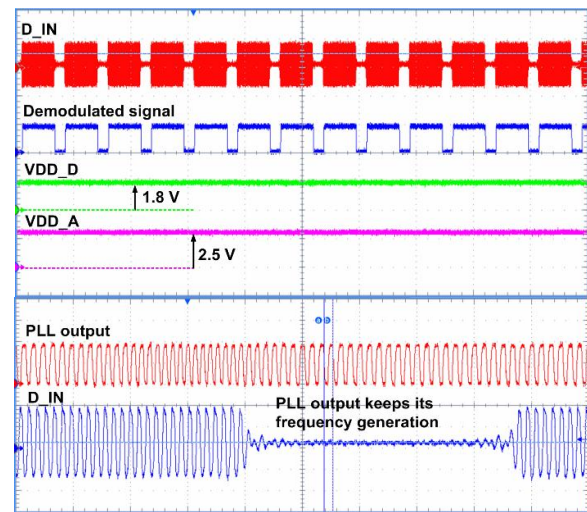


Fig. 10. The measured demodulated signal, generated power, and clock signal.

with an external coil. The chip, implemented in a 0.18  $\mu\text{m}$  CMOS process, has been basically tested in tag-to-tag response and additionally confirmed in tag-to-cellular response as shown in Fig. 9. We can verify that the signal is modulated and demodulated while PLL and LDO (2.5 V) work properly in the input signal over 6 dBm. The demodulator and LDO (1.8 V) operation has been confirmed in the input signal over 8 dBm. Fig. 10 shows the measured demodulated signal, generated power, and clock signal where demodulation of the signal in 8 dBm of input power. As shown in Fig. 10, for  $D\_IN$  is '0', PLL output provides a normal waveform and we can verify that demodulation is done in 100% ASK signal. Fig. 11 shows the measured load modulation and its spectrum. As shown in the Fig. 11, the measurement result shows the modulation depth is about 3.7% that is -28 dBc in the measured frequency spectrum.

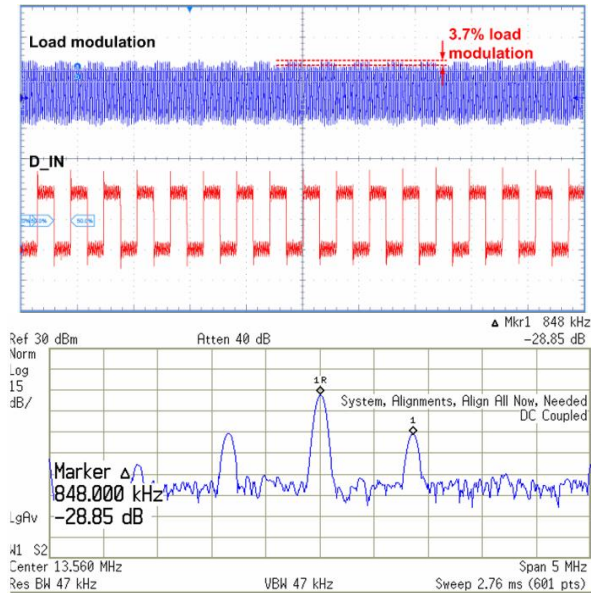


Fig. 11. The measured load modulation and its spectrum.

#### IV. CONCLUSIONS

In this paper, we propose the RF interface of NFC tag IC which is necessary for transmitting the results obtained using blood glucose sensor, water quality sensor, gas sensor and radioactive sensor to portable devices such as mobile phones. The proposed RF interface complies with the ISO14443 type-A standard using 100% ASK and solves the power and clock generation difficulties by using the internal  $V_{TH}$  canceling rectifier that is based on the high efficiency voltage doubler and the switching phase locked loop. In the measurement results, the internal  $V_{TH}$  canceling rectifier in the RF interface shows more than 80% power efficiency from 100% ASK signal, and successfully generates 1.8 V / 2.5 V supply from the input signal power higher than 6 dBm through low loss voltage regulator. Additionally, we can verify that the proposed switching phase locked loop is locked at 8 dBm or higher input signal power and successfully demodulates ASK input signal.

#### ACKNOWLEDGMENTS

This study was supported by research fund from Chosun University, 2020.

#### REFERENCES

- [1] Y. -H. Yu, Y. -J. Lee, Y. -H. Li, C. -H. Kuo, C. -H. Li, Y. -J. Hsieh, C. -T. Liu and Y. -J. E. Chen, "An LTPS TFT Demodulator for RFID Tags Embeddable on Panel Displays," IEEE Transactions on Microwave Theory and Techniques, vol. 57, no. 5, pp. 1356-1361 May 2009.
- [2] M. K. Kangi, M. M. -Nejad, and M. Nasserian, "A Fully Digital ASK Demodulator With Digital Calibration for Bioimplantable Devices," IEEE Transactions on Very Large Scale Integration (VLSI) Systems, vol. 23, no. 8, pp. 1557-1561 Aug. 2015.
- [3] G. Cai, A. Pun, D. Kwong, and KC Wang, "A 2.4pJ/bit ASK Demodulator with 100% Modulation Rate for 13.56MHz NFC/RFID Applications," IEEE International Symposium on Circuits and Systems (ISCAS), pp. 734-737 June 2014.
- [4] W. Lin, B. Geck, and H. Eul, "Optimization of NFC Compatible Transponder with Respect to the Nonlinear IC Impedance," IEEE MTT-S International Microwave Workshop on Wireless Sensing, Local Positioning, and RFID, Sept. 2009..
- [5] M. M. Ahmadi, and G. A. Jullien, "A Wireless-Implantable Microsystem for Continuous Blood Glucose Monitoring," IEEE Transactions on Biomedical Circuits and Systems, vol. 3, no. 3, pp. 169-180, June 2009.
- [6] J. -W. Lee, D. H. T. Vo, Q. -H. Huynh, and S. H. Hong, "A Fully Integrated HF-Band Passive RFID Tag IC Using 0.18-um CMOS Technology for Low-Cost Security Applications," IEEE Transactions on Industrial Electronics, vol. 58, no. 6, pp. 2531-2540 June 2010.
- [7] Y- H. Kim, Y. -C. Choi, M. -W. Seo, S. -S. Yoo, and H. -Y. Yoo, "A CMOS Transceiver for a Multistandard 13.56-MHz RFID Reader SoC," IEEE Transactions on Industrial Electronics, vol. 57, no. 5, pp. 1563-1572 May 2010.
- [8] J. -W. Lee, D. H. T. Vo, and S. H. Hong, "A Fully Integrated High Security NFC Target IC Using 0.18 um CMOS Process," IEEE European Solid State Circuits Conference pp. 551-554, Sept. 2011.
- [9] D. Nguyen, L. Nguyen, G. Thenaisie, L. Pham-Nguyen, and S. -G. Lee, "A High Power

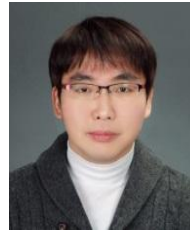
Conversion Efficiency Rectifier with New Internal  $V_{Th}$  Cancellation Topology for RFID Applications,” IEEE International Conference on Communications and Electronics, pp. 313-316, 2014.

- [10] H. Nakamoto, D. Yamazaki, T. Yamamoto, H. Kurata, S. Yamada, K. Mukaida, T. Ninomiya, T. Ohkawa, S. Masui, and K. Gotoh, “A Passive UHF RF Identification CMOS Tag IC Using Ferroelectric RAM in 0.35-um Technology,” IEEE Journal of Solid-State Circuits, vol. 42, no. 1, pp. 101-110, 2007
- [11] L. Yili, F. Xiansong, N. Pingjuan, Y. Guanghua, G. Tiecheng, “A novel CMOS current-steering amplifier based ring oscillator with the waveform shaping circuit,” IEEE International Conference on Signal Processing Systems, pp. 396-399, 2010.



**In-Young Lee** received the B.S. degree in electrical engineering from Kyungpook National University, Daegu, Korea, in 2005, and the M.S. and Ph.D. degrees in information and communications engineering from

Korea Advanced Institute of Science and Technology (KAIST), Daejeon, Korea, in 2007 and 2014 respectively. His doctoral research focused on high-frequency voltage-controlled oscillators, phase-locked loops (PLLs), and RF front-ends for digital TV tuner integrated circuits. From 2014 to 2015, he was with the Information and Electronics Research Institute, KAIST, as a post-doctoral research fellow, where he developed NFC tag ICs for smart sensors. In 2015, he joined S. LSI business, Samsung Electronics, Hwaseong, Korea focusing on low-jitter PLLs and real-time clock circuits for 5G cellular systems and IoT applications. Since fall 2017, he has been with Department of Electronic Engineering, Chosun University, Gwangju, Korea as an assistant professor. His research interests include RF/analog and mixed-mode circuit designs such as RF front-ends, PLLs, and high-frequency VCOs. Dr. Lee was the recipient of the Silver Prize and Gold Prize of the 19th and 20th Human-Tech Paper Awards of Samsung Electronics, Korea, in 2013 and 2014, respectively.



**Donggu Im** received the B.S., M.S., and Ph.D. degrees in electrical engineering and computer science from the Korea Advanced Institute of Science and Technology (KAIST), Daejeon, Korea, in 2004, 2006, and 2012, respectively. From 2006 to 2009, he was an Associate Research Engineer with LG Electronics, Seoul, Korea, where he was involved in the development of universal analog and digital TV receiver ICs. From 2012 to 2013, he was a Post-Doctoral Researcher with KAIST, where he was involved in the development of the first RF SOI CMOS technology in Korea with SOI business team in National NanoFab Center (NNFC), Daejeon, Korea. In 2013, he joined the Texas Analog Center of Excellence (TxACE), Department of Electrical Engineering, University of Texas at Dallas, as a Research Associate, where he developed ultra-low-power CMOS radios with adaptive impedance tuning circuits. In 2014, he joined the Division of Electronic Engineering, Jeonbuk National University, Jeollabuk-do, Korea, and is now an Associate Professor. His research interests are CMOS analog/RF/mm-wave ICs and system design.